

Interaction Potential of a Charged Particle in a Plane-Sphere Geometry

J. Mahanty and M. T. Michalewicz

Department of Theoretical Physics, Research School of Physical Sciences,
Australian National University, G.P.O. Box 4, Canberra, A.C.T. 2601.

Abstract

The three-dimensional potential of a charged particle tunneling between a flat metal surface and a spherical metal tip is calculated within the framework of the hydrodynamic description of metallic electrons. It is demonstrated that the inclusion of coupling of surface modes in the two electrodes, even for separations as small as 10 times the screening length in either of them, contributes less than 5% of the total potential of a point charge. Hence the potential is obtained as a superposition of contributions from a planar surface and a charge neutral, conducting sphere (and can include a simple classical term for a sphere at a fixed potential). This should enable accurate determination of three-dimensional tunnel currents in scanning tunneling microscope geometry.

1. Introduction

The successful development of the scanning tunneling microscope (STM) by the IBM Zürich group (Binnig *et al.* 1982*a*, 1982*b*, 1983; Binnig and Rohrer 1982) has stimulated vigorous research activity in recent years. This promising experimental technique has already facilitated the study of the surface structure of metals, metallic glasses and semiconductors with atomic resolution (Scheel *et al.* 1982; Binnig and Rohrer 1982; Gimzewski *et al.* 1985; Binnig *et al.* 1986*a*; Feenstra *et al.* 1986*a*, 1986*b*; Weisendanger *et al.* 1987). The effort of experimentalists led to the STM which can operate in air at ambient pressure and in liquids (Park and Quate 1986; Drake *et al.* 1986). The principle of STM operation has been utilised to build prototype instruments for scanning tunneling potentiometry (Murali and Pohl 1986) and atomic force measurements (Binnig *et al.* 1986*b*).

The problems of the tunneling conductance of electrons, the lateral resolution of the STM and other theoretical issues have been treated using the transfer matrix, perturbative or direct methods in a number of papers (Tersoff and Hamann 1983, 1985; Garcia *et al.* 1983; Feuchtwang *et al.* 1983; Baratoff 1984; Garcia and Flores 1984; Stoll *et al.* 1984; Stoll 1984). The tunneling occurs through a potential barrier consisting of the bias voltage and the 'image' potential.

The image potential arises from the interaction of the external charge with the charges induced in the metal due to the collective response of the electrons. The latter can be estimated using the hydrodynamic model which gives the response in terms of the plasmons (both surface and bulk). In the present paper we demonstrate that

the image potential of a charged particle between a flat metal surface and a spherical metal tip arises mainly from surface plasmons on the planar surface and a finite number of surface plasmons on the sphere. The coupling of the surface modes in the two electrodes has a very small effect on the potential when the minimum separation is larger than about ten times the screening length. Therefore the multiple-image method for generating the image potential (Simmons 1963*a*, 1963*b*; Miskovsky *et al.* 1981, 1982) is not necessary for dispersive metals.

In the semi-classical model of a static charge between the two electrodes, we obtain a three-dimensional axially symmetric potential, which is everywhere finite and saturates to two different values on the surfaces of the electrodes. This result resolves the problem of classical image potential divergence at the surface discussed recently in the present context by Binnig *et al.* (1984) and Payne and Inkson (1985).

A study, which addressed the same question of the charged particle potential in a model STM geometry identical with ours has just been completed by Morawitz *et al.* (1987); in this sense, our work is complementary to theirs. However, they used the classical multiple-image method which, in our opinion, limits their results to ideal conductors. On the other hand, our treatment takes into account the dynamics of the collective modes of conduction electrons, including their spatial dispersion.

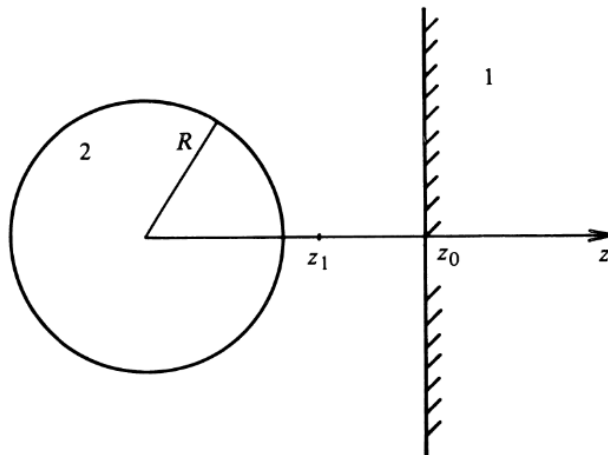


Fig. 1. Geometry of the sphere-plane coupling problem.

2. Problem of Plane-Sphere Coupling

The magnitude of the contribution to the total potential due to coupling between surface plasmons on a plane and a sphere is estimated using a general approach presented by Michalewicz and Mahanty (1986). Let us consider a metal sphere of radius R (medium 2) and a flat metal surface (medium 1) at a distance $z_0 - R$ from the surface of the sphere. The z -axis is normal to the planar surface and has its origin at the centre of a sphere. An external, stationary point charge Q is confined, for simplicity, to the axial line at z_1 , with $R \leq z_1 \leq z_0$ (see Fig. 1).

We assume that the density of conduction electrons in both metallic jellium media obeys the hydrodynamic equation of motion. In cylindrical coordinates the solutions

for the electronic densities are ($l = 1$ and $m = 0$)

$$n_{\text{sp}}(r) = D \left(\frac{3}{4\pi} \right)^{\frac{1}{2}} \cos \theta m_1(k_2 r), \quad (1a)$$

$$n_{\text{pl}}(r) = (2\pi)^{-2} \int d^2 k C(k) J_0(k\rho) \exp\{-\gamma(z-z_0)\}. \quad (1b)$$

In these expressions, $m_1(x) = (\pi/2x)^{-1/2} I_{3/2}(x)$ is the modified spherical Bessel function of the first kind and the first order, while $J_0(x)$ is the Bessel function of the first kind and the zeroth order. Further, $\gamma^2 = k^2 + k_1^2$, and k_i^{-1} is the Thomas–Fermi screening length in the i th metal, with $k_i = \omega_{\text{p}(i)}/\beta_i$, where $\omega_{\text{p}(i)}$ is the plasma frequency and β_i is the dispersion parameter. The high and low frequency values of β_i^2 are $\frac{3}{5} v_{\text{F}(i)}^2$ and $\frac{1}{3} v_{\text{F}(i)}^2$ respectively, $v_{\text{F}(i)}$ being the Fermi velocity. The density fluctuations in both media are mutually orthogonal with respect to the number m . The predominant contribution to the charged particle–metallic sphere interaction potential is due to the dipole mode ($l = 1$) and is of order $\sim (R/r)^4$ outside the sphere. The higher multipole modes contribute by terms of the smaller order $O((R/r)^6)$, where R is the radius and r is the position of the charge measured from the centre of the sphere (Mahanty and Michalewicz 1986). This justifies our choice of dipole mode on the sphere, $l = 1$, and $m = 0$ solution in the plane as the principal solutions for the density fluctuations (1a) and (1b) in the coupling problem.

The coupling occurs in the normalisation constants $C(k)$ and D which are solved from the boundary conditions. To this end we require that the normal current in metal 1 and the radial current in metal 2 vanish at the respective surfaces. This is written as

$$\left\{ -m\beta_1^2 \frac{\partial}{\partial z} n_{\text{pl}} + en_{01} \frac{\partial}{\partial z} \phi_{\text{pl}} + en_{01} \frac{\partial}{\partial z} \phi_{\text{sp}} = -\frac{\partial}{\partial z} \frac{Qen_{01}}{|r-z_1|} \right\}_{z=z_0}, \quad (2a)$$

$$\left\{ -m\beta_2^2 \frac{\partial}{\partial r} n_{\text{sp}} + en_{02} \frac{\partial}{\partial r} \phi_{\text{pl}} + en_{02} \frac{\partial}{\partial r} \phi_{\text{sp}} = -\frac{\partial}{\partial r} \frac{Qen_{02}}{|r-z_1|} \right\}_{r=R}, \quad (2b)$$

where n_{0i} is the equilibrium electron number density in the i th metal. The boundary conditions lead to equations for the coefficients

$$C(k) = A(k) + DB(k), \quad D\Gamma = \int dk \Delta(k) C(k) + \int dk A(k), \quad (3a, b)$$

where

$$A(k) = \frac{Q}{e} \omega_{\text{p1}}^2 \frac{(\gamma+k) \exp\{k(z_1-z_0)\}}{2\beta_1^2 \gamma(\gamma+k) - \omega_{\text{p1}}^2}, \quad (4a)$$

$$B(k) = -\left(\frac{4\pi}{3}\right)^{\frac{1}{2}} (\omega_{\text{p1}}^2 R^3/k_2) m_2(k_2 R) \frac{k(\gamma+k) \exp(-kz_0)}{2\beta_1^2 \gamma(\gamma+k) - \omega_{\text{p1}}^2}, \quad (4b)$$

$$\Gamma = -\frac{1}{3} m_2(k_2 R) - \frac{m_1(k_2 R)}{k_2 R}, \quad (4c)$$

$$\Delta(k) = \frac{1}{2} \left(\frac{3}{4\pi} \right)^{\frac{1}{2}} k_2 \frac{k \exp(-kz_0)}{\gamma + k} W(k, R), \quad (4d)$$

$$\Lambda(k) = -\frac{1}{2} \left(\frac{3}{4\pi} \right)^{\frac{1}{2}} \frac{Q}{e} k_2 k \exp(-kz_0) W(k, R), \quad (4e)$$

and where

$$W(k, R) = \int_0^\pi d\theta \sin \theta \cos \theta \exp(kR \cos \theta) \\ \times \{ \cos \theta J_0(kR \sin \theta) - \sin \theta J_1(kR \sin \theta) \}. \quad (5)$$

Let us now choose the units of z_0 , z_1 and R to be k_1^{-1} , and let k be in units of k_1 . This is equivalent to the change of variables $k \rightarrow k = k/k_1$, $k_1 \rightarrow 1$, $k_2 \rightarrow k_2/k_1$, $z_1 \rightarrow z_1 k_1$, $z_0 \rightarrow z_0 k_1$, $R \rightarrow R k_1$, and $\gamma \rightarrow \gamma = (k^2 + 1)^{1/2}$. Now, the coefficient D is found to be

$$D = \frac{1}{2} \left(\frac{3}{4\pi} \right)^{\frac{1}{2}} \frac{Q}{e} k_1^2 k_2 (I_1 - I_2) / \{ \Gamma + \frac{1}{2} R^3 m_2(k_2 R) I_3 \}, \quad (6)$$

where the dimensionless integrals I_1 , I_2 and I_3 are

$$I_1 = \int_0^\infty dk k \frac{\exp\{-k(2z_0 - z_1)\}}{2\gamma(\gamma + k) - 1} W(k, R), \quad (7a)$$

$$I_2 = \int_0^\infty dk k \exp(-kz_1) W(k, R), \quad (7b)$$

$$I_3 = \int_0^\infty dk k^2 \frac{\exp(-2kz_0)}{2\gamma(\gamma + k) - 1} W(k, R). \quad (7c)$$

It is interesting to note that the expressions (6), (7a) and (7c) are solved analytically in the dispersionless case ($\beta \rightarrow 0$, $\gamma \rightarrow 1$). The integral I_1 takes, then, the form of I_2 :

$$I(\alpha) = \int_0^\infty dk k \exp(-k\alpha) W(k, R) = \frac{2}{3} \alpha^{-2}, \quad (8)$$

and

$$I_3(\beta = 0) = \frac{d}{d\alpha} I \Big|_{\alpha=2z_0}. \quad (9)$$

Hence, in the *dispersionless case* we have

$$I_1 = \frac{2}{3} (2z_0 - z_1)^{-2}, \quad (10)$$

$$I_2 = \frac{2}{3} z_1^{-2} \quad \text{in all cases,} \quad (11)$$

$$I_3 = -\frac{4}{3} (2z_0)^{-3}, \quad (12)$$

and, using (10)–(12), all subsequent expressions lead to the multiple-image type of

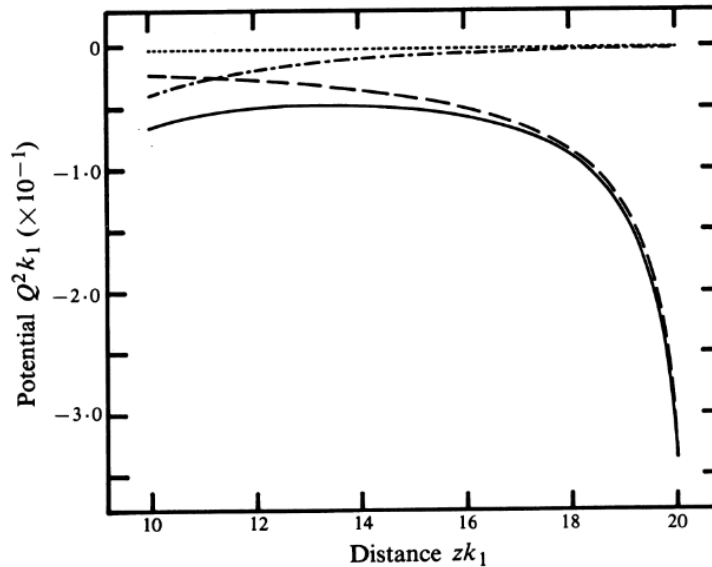


Fig. 2. Potential barrier along the axial line in the coupled sphere (W)–plane (Ag) problem. The geometry is as depicted in Fig. 1. The surface of the sphere is at $z k_1 = 10$ and the surface of the plane at $z k_1 = 20$. The distance z is in units of the Thomas–Fermi screening length in the sample, $k_1^{-1} = a_0(r_S/2.44355)^{1/2}$ and the energy units are $Q^2 k_1 = 2 a_0 k_1$ (Ry). The solid curve represents the total potential, the dashed curve the contribution from the plane, the dash–dot curve the contribution from the dipole mode on the sphere, and the dotted curve the coupling contribution ($< 5\%$ of total).

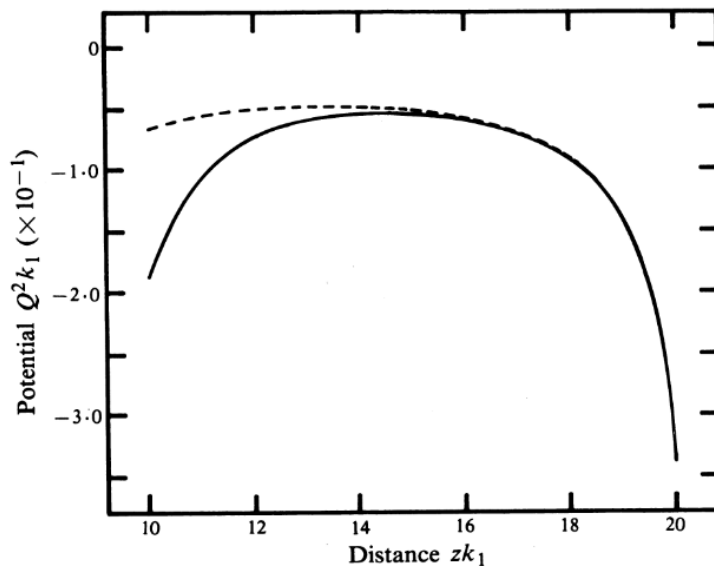


Fig. 3. Potential of a charged particle along the axial line in a sphere–plane geometry including all surface modes on the sphere (solid curve) and only the dipole mode (dashed curve). The units and geometry are as in Fig. 2.

result (divergent at the surface of the plane). To recover full multiple-image interaction energy one has also to sum all the higher modes on the dispersionless sphere.

The induced potential in the sphere–plane system is

$$\begin{aligned} \phi_1(r) = \phi_{pl}(r) + \phi_{sp}(r) = & -\frac{e}{2\pi} \int \frac{d^2k}{k} \frac{C(k) J_0(k\rho) \exp\{k(z-z_0)\}}{\gamma+k} \\ & - \left(\frac{4\pi}{3}\right)^{\frac{1}{2}} e \frac{m_2(k_2 R)}{k_2} D R^3 \frac{\cos \theta}{r^2}, \end{aligned} \quad (13)$$

and, consequently, the self-energy of a charge Q is

$$\begin{aligned} \Sigma(z_1) = \frac{Q}{2} \phi_1(z_1) = & -\frac{Q^2 k_1}{2} \int dk \frac{\exp\{2k(z_1-z_0)\}}{2\gamma(\gamma+k)-1} \\ & + \frac{Q^2 k_1}{2} \frac{m_2(k_2 R)}{2} \frac{R^3}{z_1^2} I_2/\Gamma + \text{CT}. \end{aligned} \quad (14)$$

The first and second terms in (14) are respectively the classical interaction potential of a charged particle with the dispersive plane and the dispersive sphere with only dipole mode present. The coupling term is

$$\begin{aligned} \text{CT} = \frac{Q^2 k_1}{2} \frac{m_2(k_2 R)}{2} \frac{R^3}{z_1^2} & \left((I_1 - I_2) I_4 z_1^2 + \frac{m_2(k_2 R)}{2} R^3 I_2 I_3 + \Gamma I_1 \right) \\ & \times \left\{ \Gamma \left(\Gamma + R^3 \frac{m_2(k_2 R)}{2} I_3 \right) \right\}^{-1}, \end{aligned} \quad (15)$$

and the integral I_4 is

$$I_4 = \int_0^\infty dk k \frac{\exp\{-k(2z_0-z_1)\}}{2\gamma(\gamma+k)-1}. \quad (16)$$

The interaction potential $\Sigma(z_1)$ and its separate contributions are depicted in Fig. 2. The most important result is that the correction term does not exceed 5% of the total potential. In obtaining these results we used the expressions (7) in the general case of dispersive media. Fig. 3 shows the potential of a charged particle in a plane–sphere geometry, along the axial line, when all the higher surface modes are included (in the example at hand there are six surface modes).

Inclusion of all modes on the sphere in our computation of the coupling term would result in a considerable computational complication, since then a bigger matrix equation, instead of (3), would have to be solved. However, since the coupling terms with higher modes of the sphere diminish rapidly with the plane–sphere distance of separation, we conclude that the coupling contributions for all higher modes will not be higher than $\sim 5\%$ of the principal decoupled plane and multipole terms.

3. Plane–Sphere Potential Barrier

The potential of a static charge Q , tunneling between a metal plane and a spherical tip, is constructed as a superposition of decoupled contributions from the sphere and the plane. It is a matter of straightforward application of the method presented by

Michalewicz and Mahanty (1986) to obtain the potential in a charge-plane system

$$\Sigma_{\text{pl}}(z) = -\frac{Q^2 k_1}{2} \int_0^\infty dk \exp(-2kz)/(\gamma + k)^2, \quad (17)$$

where z is measured from the planar surface in units of k_1^{-1} and $\gamma = (k^2 + 1)^{1/2}$.

The calculation of the potential in a charge-sphere system is a more involved problem and has been exhaustively treated by Mahanty and Michalewicz (1986). As observed therein, the contribution from the bulk modes can be ignored outside the sphere, and then the potential is written as (Mahanty and Michalewicz 1986, eq. 40a)

$$\Sigma_{\text{sp}}(r) = -\frac{Q^2 k_1}{2R} \sum_{l=1}^{l_{\text{max}}} \frac{\omega_p^2}{\omega_l^2} \frac{1}{(2l+1)\Delta_l^s} \left(\frac{R}{r}\right)^{2(l+1)}; \quad r > R, \quad (18)$$

where ω_l are the eigenfrequencies of the surface modes, which are found from the dispersion equation

$$\frac{m_l(kR)}{kR} = \left\{ 1 - \left(\frac{2l+1}{l+1} \right) \frac{k^2}{k_2^2} \right\} \frac{m'_l(kR)}{l}; \quad k^2 = \frac{\omega_p^2 - \omega^2}{\beta^2}, \quad (19)$$

and $k_2^2 = \omega_{\text{p}(2)}^2/\beta_2^2$. Here l_{max} is the number of surface modes on the sphere, $l_{\text{max}} \approx \{(36 + 16y^2)^{1/2} - 6\}/8$ with $y^2 = k_2^2 R^2$, and Δ_l^s is defined through equation (31) in Mahanty and Michalewicz (1986). Further, $m_l(x) = (\pi/2x)^{-1/2} I_{l+1/2}(x)$ are the modified spherical Bessel functions.

The results for the interaction potential computed from (18) were tabulated for the sizes of the sphere $R \in \{10, 20, 50, 100\}$ and for different metals represented by a parameter $k_2/k_1 \in \{1.0, 1.1, 1.2, 1.3, 1.4\}$; the value of k_1 was taken for Ag.*

The principal results of this work are depicted in Figs 4 and 5. Figs 4a and 5a show the axially symmetric potential barrier in the tip-sample geometry for the two inter-electrode separations $10k_1^{-1}$ and $20k_1^{-1}$ respectively. The three-dimensional relief of the barrier is presented in Figs 4b and 5b for the same two separations. The barrier is much lower for the narrower tip-sample gap. This is an important effect which might show up in the onset of tunneling at the fixed applied bias; it has not received much attention so far.

It should be pointed out that the metal tip in our model is the charge neutral, insulated, conducting sphere. In order to include the effect of a fixed potential V at the surface of the sphere the classical term (Jackson 1975) $\Sigma_V(r) = VRQ/2r$ should be added to (18).

4. Conclusions

In the present work we have calculated the interaction potential of a stationary point charge in the model scanning tunneling microscope geometry. The sample has been taken as a flat free-electron jellium metal, and the probing tip has been modelled by a charge neutral, insulating, conducting sphere. It has been assumed that the conduction electrons obey the hydrodynamic equation of motion. In most experimental situations the probing tip is made of tungsten, although other metals such as iridium and molybdenum have been used. Smith (1969) pointed out that

* These tables are available from the authors on request.

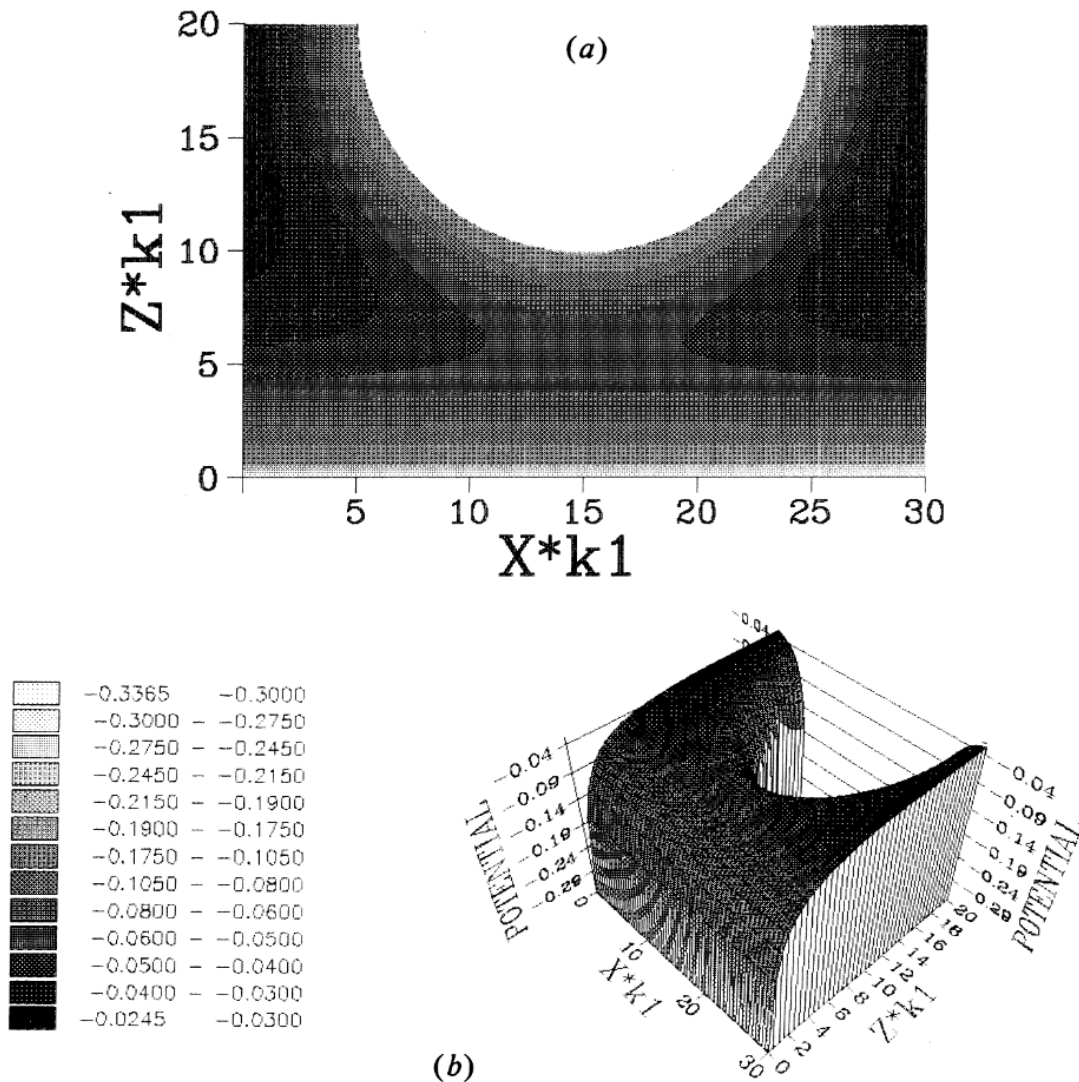


Fig. 4. (a) Induced potential contours of a charged particle in the model STM. The probe (W)-sample (Ag) separation is $10k_1^{-1}$. The units are the same as in Fig. 2. (b) The potential barrier of Fig. 4a as a three-dimensional relief.

many surface properties of the transition metals are successfully described within the free-electron model, and certainly his calculations of the work functions and surface potentials show good agreement with experiment. Assured by this agreement we have treated the sphere as being jellium and free-electron-like, with the effective Wigner-Seitz radius for tungsten of $r_s = 1.62$ (Mehrotra 1979). The only parameters of the theory are therefore the electronic densities in the probe and the sample.

We have demonstrated that coupling of the surface modes in the two electrodes has a negligible effect on the potential barrier for the typical separations encountered in experiments, of the order of 10 times the Thomas-Fermi screening length. The coupling contributes less than 5% to the total potential and hence can be ignored.

In principle, the shape of the tunneling potential barrier can be estimated in the same manner as done here if the independent potentials due to the plane and the sphere are obtained by other methods. There are many estimates in the literature of the image potential due to a plane, using other methods such as the density functional method (Appelbaum and Hamann 1972; Lang and Kohn 1973) or the dielectric

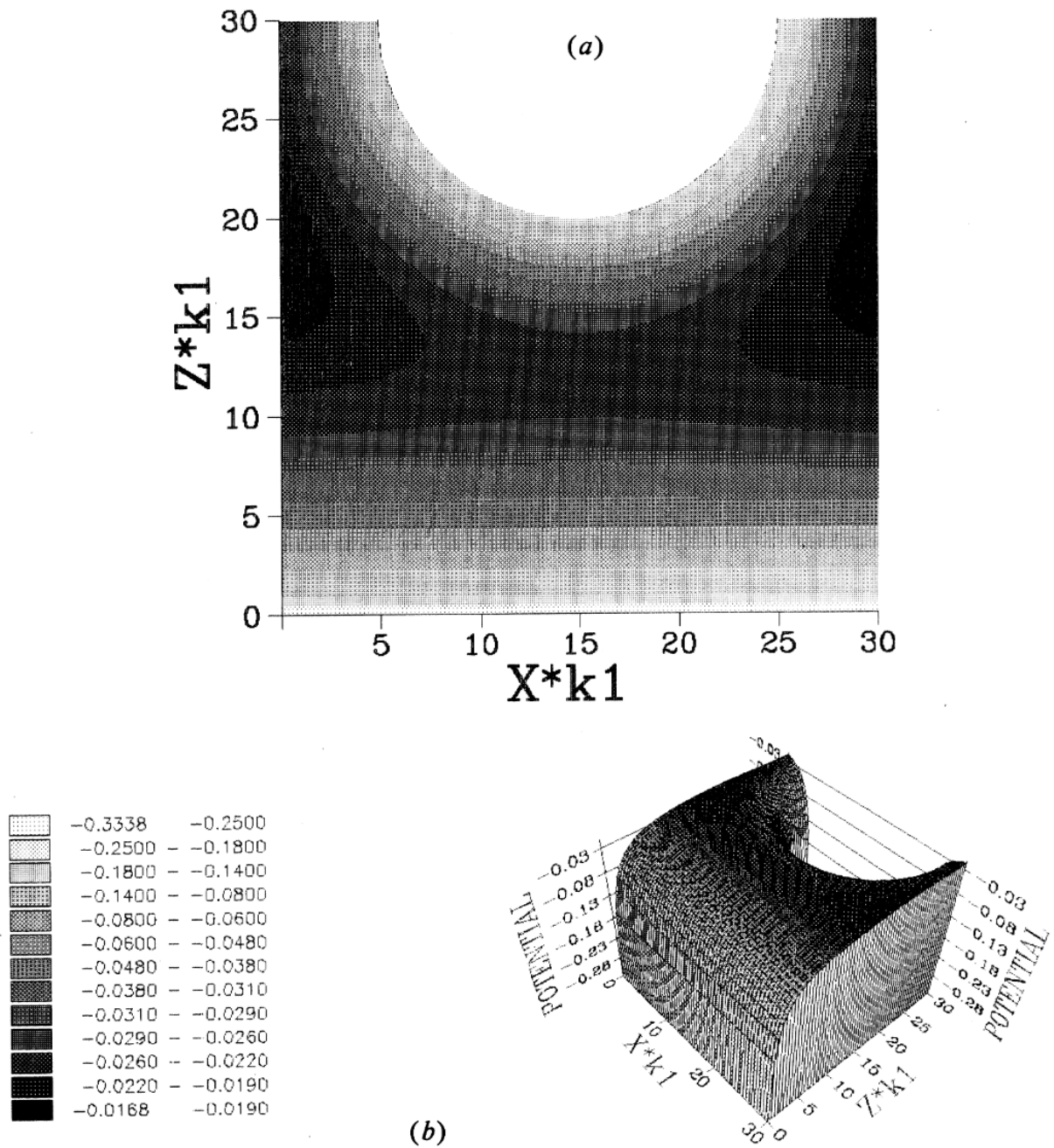


Fig. 5. The same as Fig. 4 but for a separation of $20k_1^{-1}$. Note the lowering of the barrier.

response method (Equiluz *et al.* 1984). Similar calculations for the image potential due to a sphere are not available to the best of our knowledge.

The effective potential barrier in a plane-sphere geometry has an obvious rotational symmetry about the line normal to the surface and joining the centre of the sphere. It displays a 'valley' centred along the axial line where strong enhancement of the tunnel current should be expected. The spherical model of the tip shows that STM is an excellent local probe of the electronic structure of the sample, since the tunnel current will decrease rapidly in lateral distances of about half the tip radius. This effect has been discussed by Morawitz *et al.* (1987). The inadequacy of the one-dimensional theory of tunneling and the need for a three-dimensional description of the STM operation is evident from our results.

References

- Appelbaum, J. A., and Hamann, D. R. (1972). *Phys. Rev. B* **6**, 1122.
- Baratoff, A. (1984). *Physica B* **127**, 143.
- Binnig, G., Fuchs, H., Gerber, Ch., Rohrer, H., Stoll, E., and Tossati, E. (1986a). *Europhys. Lett.* **1**, 31.
- Binnig, G., Garcia, N., Rohrer, H., Soler, J. M., and Flores, F. (1984). *Phys. Rev. B* **30**, 4816.
- Binnig, G., Quate, C. F., and Gerber, Ch. (1986b). *Phys. Rev. Lett.* **56**, 930.
- Binnig, G., and Rohrer, H. (1982). *Helv. Phys. Acta* **55**, 726.
- Binnig, G., Rohrer, H., Gerber, Ch., and Weibel, E. (1982a). *Appl. Phys. Lett.* **40**, 178.
- Binnig, G., Rohrer, H., Gerber, Ch., and Weibel, E. (1982b). *Phys. Rev. Lett.* **49**, 57.
- Binnig, G., Rohrer, H., Gerber, Ch., and Weibel, E. (1983). *Phys. Rev. Lett.* **50**, 120.
- Drake, B., Sonnenfeld, R., Schreier, J., Hansma, P. K., Slough, G., and Coleman, R. V. (1986). *Rev. Sci. Instrum.* **57**, 441.
- Equiluz, A. G., Campbell, D. A., Maradudin, A. A., and Wallis, R. F. (1984). *Phys. Rev. B* **30**, 5449.
- Feenstra, R. M., Thompson, W. A., and Fein, A. P. (1986a). *Phys. Rev. Lett.* **56**, 608.
- Feenstra, R. M., Thompson, W. A., and Fein, A. P. (1986b). *J. Vac. Sci. Technol. A* **4**, 1315.
- Feuchtwang, T. E., Cutler, P. H., and Miskovsky, N. M. (1983). *Phys. Lett. A* **99**, 167.
- Garcia, N., and Flores, F. (1984). *Physica B* **127**, 137.
- Garcia, N., Ocal, C., and Flores, F. (1983). *Phys. Rev. Lett.* **50**, 2002.
- Gimzewski, J. K., Humbert, A., Bednorz, J. G., and Reihl, B. (1985). *Phys. Rev. Lett.* **55**, 951.
- Jackson, J. D. (1975). 'Classical Electrodynamics', 2nd edn, p. 60 (Wiley: New York).
- Lang, N. D., and Kohn, W. (1973). *Phys. Rev. B* **7**, 3541.
- Mahanty, J., and Michalewicz, M. T. (1986). *J. Phys. C* **19**, 5005.
- Mehrotra, R. (1979). Ph.D. Thesis, Aust. Nat. Univ.
- Michalewicz, M. T., and Mahanty, J. (1986). *Phys. Lett. A* **116**, 392.
- Miskovsky, N. M., Cutler, P. H., and Feuchtwang, T. E. (1981). *Int. J. Infrared Mill. Wav.* **2**, 739.
- Miskovsky, N. M., Cutler, P. H., and Feuchtwang, T. E. (1982). *Appl. Phys. A* **27**, 139.
- Morawitz, H., Batra, I. P., Reinish, R., and Henry, G. R. (1987). *Surf. Sci.* **180**, 333.
- Muralt, P., and Pohl, D. W. (1986). *Appl. Phys. Lett.* **48**, 514.
- Park, S., and Quate, C. F. (1986). *Appl. Phys. Lett.* **48**, 112.
- Payne, M. C., and Inkson, J. C. (1985). *Surf. Sci.* **159**, 485.
- Scheel, H. J., Binnig, G., and Rohrer, H. (1982). *J. Cryst. Growth* **60**, 199.
- Simmons, J. G. (1963a). *J. Appl. Phys.* **34**, 1793.
- Simmons, J. G. (1963b). *J. Appl. Phys.* **34**, 2581.
- Smith, J. R. (1969). *Phys. Rev.* **181**, 522.
- Stoll, E. (1984). *Surf. Sci.* **143**, L411.
- Stoll, E., Baratoff, A., Selloni, A., and Carnevali, P. (1984). *J. Phys. C* **17**, 3073.
- Tersoff, J., and Hamann, D. R. (1983). *Phys. Rev. Lett.* **50**, 1998.
- Tersoff, J., and Hamann, D. R. (1985). *Phys. Rev. B* **31**, 805.
- Weisendanger, R., Ringger, M., Rosenthaler, L., Hidber, H. R., Oelhafen, P., Rudin, H., and Grüntherodt, H. J. (1987). *Surf. Sci.* (in press).